

DESIGN OF A 250 MeV, X-BAND PHOTOINJECTOR LINAC FOR A PRECISION COMPTON-SCATTERING BASED GAMMA-RAY SOURCE*

S. G. Anderson[†], F. Albert, D. J. Gibson, D. McNabb, M. Messerly, B. Rusnak, M. Shverdin,
F. V. Hartemann, C. W. Siders, C. P. J. Barty, LLNL, Livermore, CA 94550, USA
S. Tantawi, A. Vlieks, SLAC, Menlo Park, CA 94025, USA

Abstract

We present a compact, X-band, high-brightness accelerator design suitable for driving a precision gamma-ray source. Future applications of gamma-rays generated by Compton-scattering of laser and relativistic electron beams place stringent demands on the brightness and stability of the incident electron beam. This design identifies the beam parameters required for gamma-ray production, including position, and pointing stability. The design uses an emittance compensated, 11.4 GHz photo-gun and linac to generate 400 pC, 1-2 mm-mrad electron bunches at up to 250 MeV and 120 Hz repetition rate. The effects of jitter in the RF power system are analyzed as well as structure and optic misalignments. Finally, strategies for the mitigation of on-axis Bremsstrahlung noise are discussed.

INTRODUCTION

Bright, narrow bandwidth gamma-ray sources based on Compton scattering of laser pulses with ultra-relativistic electron beams have recently been used to excite Nuclear Resonance Fluorescence (NRF) lines in various isotopes [1, 2]. Applications of isotope specific detection based on excitation of NRF by Compton sources are under investigation at LLNL, and include homeland security, waste identification, and material characterization.

Common to all of the proposed NRF applications is the need for high average photon flux at a specified energy (i.e., to maximize $N_\gamma/eV/sec$ at the NRF resonances line) while concurrently minimizing background noise from off-resonance radiation. For the Compton source, these requirements motivate the use of small laser and electron beam sizes, σ_x , at the interaction point (IP) to increase flux, yet maintain a small normalized beam divergence, $\gamma\sigma_{x'}$, to decrease the bandwidth of the γ -rays.

The effect of electron beam divergence on source bandwidth can be seen through the expression for scattered photon energy in the Thomson limit (where $\gamma E_L \ll m_e c^2$),

$$E_\gamma \approx 2\gamma^2 E_L \frac{1 + \cos \phi}{1 + \gamma^2 \theta^2}, \quad (1)$$

where ϕ is the angle between electron and incident photon, defined such that $\phi = 0$ for a head-on collision, and θ is the observation angle with respect to the electron direction. If

we consider the head-on collision geometry, then the angles are defined with respect to the electron beam axis, and $\phi = \theta$ is the small angle made by an electron with respect to the beam axis due to non-zero emittance. Then Eq. 1 can be expanded to give

$$\left. \frac{\Delta E_\gamma}{E_\gamma} \right|_{\text{on-axis}} = \frac{\Delta E_L}{E_L} + \frac{2\Delta\gamma}{\gamma} - \gamma^2 \Delta\theta^2. \quad (2)$$

In a more rigorous analysis [3], it has been shown that, in summing over the beam, the terms in Eq. 2 add in quadrature to give the γ -ray source bandwidth. The final term corresponds with the square of the normalized beam divergence, or $\varepsilon_n^2/\sigma_x^2$. Because this expression involves the *normalized* emittance, a high brightness beam is required to efficiently scatter photons while maintaining a narrow bandwidth. Tolerance to electron beam pointing jitter at the IP can also be evaluated using Eq. 2. Over multiple shots, errors in electron beam pointing will increase the effective beam divergence and therefore increase source bandwidth:

$$\Delta\theta_{\text{eff}}^2 = \sigma_{x'}^2 + \theta_{\text{jitter},rms}^2 \quad (3)$$

In the accelerator design described below, we choose as a goal $\theta_{\text{jitter},rms} < 0.2\sigma_{x'}$, to keep the effect of pointing jitter negligible. A similar constraint on position jitter is chosen to minimize growth of the effective spot size at the IP.

INJECTOR BEAM DYNAMICS

The 250 MeV linac design begins with a 5.5 cell X-band photo-gun to be built by a collaboration between LLNL and SLAC. The gun design is based on a previous SLAC gun [4] which was operated with 200 MV/m peak accelerating field, and generated 0.5 nC, 7 MeV bunches [5]. Beam parameters are chosen partially by scaling the design of the S-band, T-REX (Thomson-Radiated Extreme X-rays) photoinjector [6]. The ideal design scaling of lengths with λ_{RF} and fields with λ_{RF}^{-1} [7] would require 480 MV/m electric field on the photo-cathode. In the present case, the beam plasma wavenumber, $k_p = \sqrt{4\pi r_e n_b / \gamma^3}$, where r_e is the classical electron radius and n_b is the beam density, is scaled with the increase in anticipated field strength from the S-band system (a factor of 5/3). To maintain an RF curvature induced energy spread of a few times 10^{-3} , the pulse length is set at 10 degrees of RF phase, scaled strictly with frequency. A bunch charge of 400 pC was selected with transverse size at the cathode chosen to produce the

Light Sources and FELs

A05 - Synchrotron Radiation Facilities

* This work performed under the auspices of the U.S. Department of Energy by Lawrence Livermore National Laboratory under Contract DE-AC52-07NA27344

[†] anderson131@llnl.gov

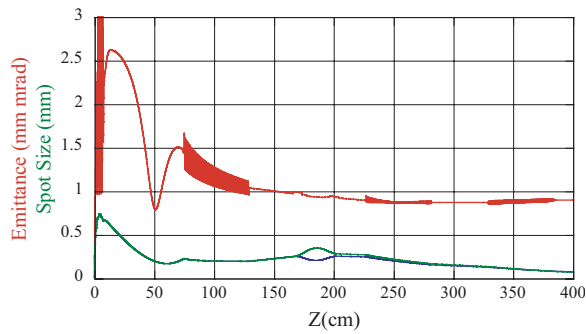


Figure 1: PARMELA simulation showing the horizontal emittance and rms beam size in the photo-gun and three following traveling-wave sections.

desired k_p . Also scaling with k_p is the drift distance from gun to linac section, chosen in this case to be 80 cm.

A PARMELA [8] simulation of the injector is shown in Fig. 1. The well developed emittance compensation technique [9] is employed to produce an emittance minimum before injection into the first linac section where acceleration arrests the space-charge emittance oscillation at a second emittance minimum of just under $1 \mu\text{m}$, rms, normalized. The accelerator uses 6 X-band traveling-wave sections of type T53VG3 [10], developed by SLAC in a program for International Linear Collider structure R&D. These 60 cm, $2\pi/3$ phase advance per cell structures are simulated with an accelerating gradient just below 80 MV/m, limited by anticipated RF power availability. Although Fig. 1 shows the beam evolution through only three sections, the emittance and spot sizes are essentially unchanged by the following sections, and the simulated final beam energy is 267 MeV.

BEAM TRANSPORT

The key issues addressed in the design of the beam transport lattice from the exit of the linac to the Compton-scattering IP are emittance preservation, mitigation of on-axis Bremsstrahlung, and incorporation of the interaction laser into the final-focus optical system. In previous Compton source development work at LLNL, unwanted background radiation limited the utility of many of the γ -ray beam diagnostics employed. This radiation was observed to be effectively on-axis (i.e., only partially removed by collimation), unchanged by absence of photo-beam, and eliminated by removing RF power in the photo-gun. Spectral measurements were performed using a high-purity Germanium detector, which showed the radiation to be broadband, and extending upwards of 8 MeV (detector range limited). From this evidence, the noise source is determined to be Bremsstrahlung produced by dark current electrons generated in the gun and striking the walls of the accelerator and vacuum system downstream.

The increase in photo-cathode peak field in the planned machine, and its associated increase in dark current, makes

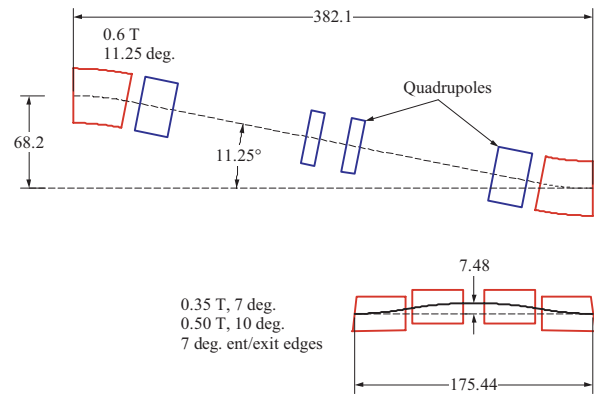


Figure 2: Dog-leg and chicane geometries studied in ELEGANT simulations. Dimensions are in cm.

the removal of the anticipated on-axis Bremsstrahlung an important lattice design consideration. The dog-leg and chicane geometries are examined here. We investigate the designs shown in Fig. 2. Both the dog-leg and chicane beamlines offer methods to shield radiation on the linac axis, while terminating dispersion-free ($\eta = \eta' = 0$). While the dog-leg design offsets the γ -ray beam from the linac axis, and offers better potential for shielding, it is less compact, requires strong focusing, and is operationally less robust than the chicane. The chicane also has the advantage that it can be disabled to allow straight through operation if desired. While either lattice may be used for bunch compression, this design focuses on emittance preservation.

To investigate the effect of coherent synchrotron radiation (CSR) on emittance in these two cases, phase space distributions were taken from PARMELA simulations of the linac and fed into the code ELEGANT [11]. In the simulation of both systems a quadrupole triplet is inserted after the final linac section for proper matching into the bend lattice. Two more sets of focusing triplets follow, the last providing the final focus to the IP. The simulated beam sizes and final focus configuration space is shown for the dog-leg geometry in Fig. 3. The final bend plane (x) emittance increases slightly with inclusion of CSR in the simulation from 1.4 to $1.9 \mu\text{m}$, rms. This growth can be seen as an asymmetric tail in the configuration space.

Two different chicane geometries were simulated, the first using 2 meter radius of curvature, 15° bends, and the second using 3.09 meter radius and 7° bends. In each case a 15 cm drift is set between the center magnets for insertion of on-axis shielding material. The final focus configuration space for each case is shown in Fig. 4. In the case with larger bend angles there is significant CSR induced emittance growth to $3.2 \mu\text{m}$, while for the smaller chicane, no emittance growth is observed. The advantages of chicane beamlines mentioned above and effective emittance preservation of the small chicane motivate use of this design over the dog-leg.

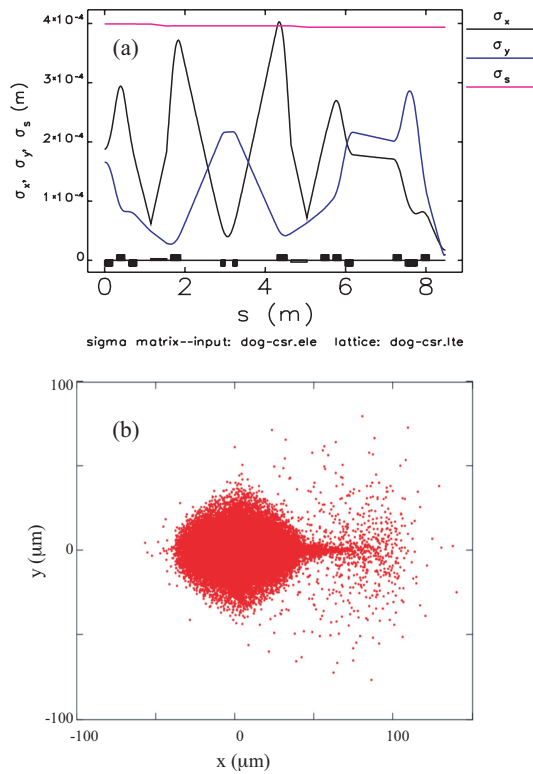


Figure 3: ELEGANT simulation of (a) the beam sizes and (b) final focus configuration space for the dog-leg lattice.

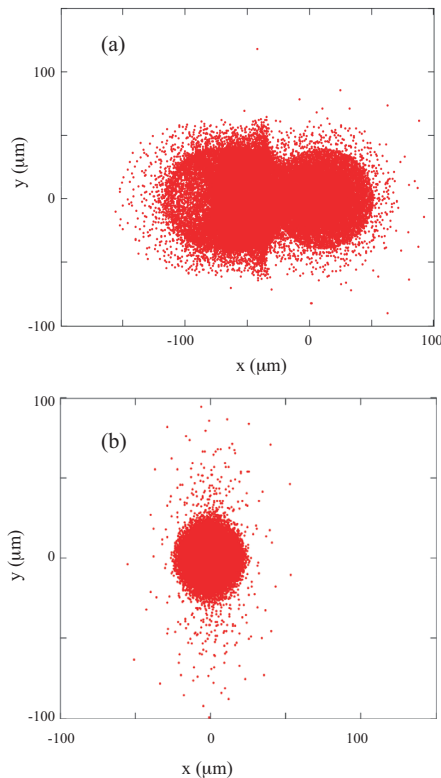


Figure 4: ELEGANT simulations of the final focus configuration space for chicane lattices with (a) 5.4 kG and 15° bends, and (b) 3.5 kG and 7° bends.

ALIGNMENT AND JITTER

As mentioned above, rms position and pointing jitter should not exceed roughly 20% of respective bunch dimensions at the IP to avoid appreciable decrease in the photon source brightness. In the cases considered here, the IP sizes are $\sigma_x = 20\mu\text{m}$, and $\sigma_{x'} = 0.2\mu\text{rad}$, indicating a desired jitter below $4\mu\text{m}$ and $40\mu\text{rad}$, respectively.

A series of ELEGANT simulations has been performed to determine the effect of various random errors on the beam first and second moments at the IP. Jitter in beam position and pointing at the lattice entrance, ground motion induced jitter in magnet position, and magnet misalignments were all simulated in batch runs of 400 to give 5% statistics on the resulting jitter figures, summarized in Table 1. The simulations show that beam pointing stability from the accelerator is required to be on the order of $1\mu\text{rad}$. This can be accomplished with 10^{-3} linac energy jitter and steering due to misaligned elements kept on the order of 1 mrad.

Table 1: Jitter Simulation Results

Varied Input Parameter	IP Jitter
$\sigma_{\langle x \rangle} = 12\mu\text{m}$	$\sigma_{\langle x \rangle} = 3\mu\text{m}$
$\sigma_{\langle x' \rangle} = 1.5\mu\text{rad}$	$\sigma_{\langle x' \rangle} = 6\mu\text{rad}$
$1\mu\text{m}$ magnet offsets	$\sigma_{\langle x \rangle} = 3.6\mu\text{m}$ $\sigma_{\langle x' \rangle} = 2.4\mu\text{rad}$
$250\mu\text{m}$ magnet misalignment	negligible ϵ increase

REFERENCES

- [1] N. Pietralla, *et al.*, Phys. Rev. Lett. **88**, 012502 (2002).
- [2] F.V. Hartemann, *et al.*, these proceedings.
- [3] Winthrop J. Brown and Frederic V. Hartemann, Phys. Rev. ST Accel. Beams **7**, 060703 (2004).
- [4] A. Vliet, *et al.*, in *High Energy Density and High Power RF: 5th Workshop AIP CP625* p. 107 (2002).
- [5] A. Vliet, *et al.*, in *High Energy Density and High Power RF: 6th Workshop AIP CP691* p. 358 (2003).
- [6] S.G. Anderson, *et al.*, in *Proceedings of PAC07*, p. 1242 (2007).
- [7] J. Rosenzweig and E. Colby, in *Advanced Accelerator Concepts, Sixth Workshop AIP CP335* p. 724 (1995).
- [8] L. Young and J. Billen, Tech. Rep. LA-UR-96-1835, LANL (1996).
- [9] B.E. Carlsten, Nucl. Instrum. Methods Phys. Res. Sect. A **285**, 313 (1989); L. Serafini and J.B. Rosenzweig, Phys. Rev. E **55** 7565 (1997).
- [10] J.W. Wang, Tech. Rep. SLAC-PUB-13554, SLAC (2009).
- [11] M. Borland, Tech. Rep. LS-287, Advanced Photon Source, (2000).